



ELSEVIER

Physica D 121 (1998) 263–274

PHYSICA D

Similarity solutions in the theory of curvature driven diffusion along planar curves: I. Symmetric curves expanding in time

Sergey Asvadurov, Bernard D. Coleman*, Richard S. Falk, Maher Moakher

Graduate Program in Mechanics and Department of Mathematics, Rutgers University, Piscataway, NJ 08854-8058, USA

Received 26 May 1997; received in revised form 1 March 1998; accepted 20 April 1998

Communicated by J.M. Ball

Abstract

A numerical method is developed for obtaining similarity solutions of the differential equations governing the evolution of a planar curve in the theory of diffusion along curves. The method is applied to cases in which the solution can be interpreted as describing the subsequent evolution (by curvature driven surface diffusion) of the boundary of a three-dimensional body that in the limit $t \rightarrow 0+$ has a form close to that of a wedge with angle of aperture 2Φ . In the theory of curvature driven evaporation, the analogous problem can be solved analytically, and hence the relation between t , Φ , and the retraction of the wedge tip can be rendered explicit. Although the differential equations of the two theories are of different orders and have solutions that differ in such qualitative properties as preservation of convexity and conservation of volume, it is found that the explicit expressions obtained for the retraction of a wedge tip by curvature driven evaporation can be transformed by rescaling into expressions that appear to be in perfect agreement with numerical results for retraction of the tip by curvature driven diffusion. © 1998 Elsevier Science B.V. All rights reserved.

PACS: 68.35.Fx

Keywords: Surface diffusion; Similarity solutions

1. Curvature driven diffusion along curves

The theory of curvature driven diffusion in the surface S of an isotropic body B is based on, (i) the constitutive equation [1,2],

$$\mathbf{q} = -K \nabla_S H, \quad (1.1)$$

which relates the mass flux \mathbf{q} in S to the surface gradient of the sum H of the principal curvatures of S , and (ii) the mass-balance equation [2],

$$\rho v + \text{div}_S \mathbf{q} = 0, \quad (1.2)$$

which relates the surface divergence of \mathbf{q} to the rate v of advance of S along its exterior normal. The material constant K is proportional to the coefficient for self-diffusion in S ; ρ is the (constant) mass density of B .

From this point on we shall assume that a characteristic length L has been specified, and we shall use, instead of such variables with dimension of length as x , y , etc., the dimensionless variables x/L , y/L , etc., and, instead of the time t , the dimensionless variable $Kt/\rho L^4$. The new variables also will be denoted by x , y , t , etc.

Eqs. (1.1) and (1.2) yield (in the new variables)

$$v = \Delta_S H \quad (1.3)$$

* Corresponding author. E-mail: bcoleman@stokes.rutgers.edu

and are said to govern the theory of *motion by Laplacian of curvature*. That theory has a less developed literature than the *theory of motion by curvature* [3], based on the equation $v = -kH$. Whereas H is given by second-order derivatives of surface coordinates, $\Delta_S H$ depends on fourth-order derivatives of such coordinates, and this fact has the consequence that a maximum principle employed in the theory of motion by curvature does not hold for (1.3). Of some interest in materials science is the related fact that a theorem of Huisken [4] in the theory of motion by curvature, to the effect that a surface convex at one time remains convex at all later times, does not hold in the theory of motion by Laplacian of curvature.

We here discuss a particular class of solutions of Eq. (1.3), namely, similarity solutions for cases in which B is a two-dimensional body that in each of its configurations occupies a (not necessarily bounded) region of a fixed plane P ; in such cases the boundary S is a planar curve $C(t)$.

The emphasis in the present paper will be on similarity solutions for which $C(t)$ represents the boundary of a body that in the past has had a shape close to that of a wedge W with angle of aperture 2Φ . One can imagine a wedge that is evolving by curvature driven surface diffusion in accord with the constitutive Eq. (1.1), or by curvature driven evaporation and condensation in accord with the relation $v = -kH$. (We shall refer to the latter theory as the theory of ‘curvature driven evaporation’, because the solutions we shall consider of the equation $v = -kH$ will be such that H is of fixed sign.) For curvature driven diffusion, the subject emphasized here, we shall present, in Section 2 below, a numerical method for finding $C(t)$, and we shall calculate the retraction of the tip of the wedge as a function of t and Φ . In Section 3 we shall show that the corresponding problem in the theory of curvature driven evaporation can be solved explicitly, and we shall observe that, although the two theories yield qualitatively different shapes for the curves $C(t)$, there is a rescaling that transforms the explicit expression for the retraction of the wedge tip obtained in the latter theory into a formula that appears to be in perfect accord with numerical results for the retraction in the former theory.

In general, when discussing the temporal evolution of a curve $C(t)$, we write $\mathbf{x} = \mathbf{x}(s, t)$ for the location in the plane P of the point of $C(t)$ with arc-length

coordinate s . The unit tangent and normal vectors of $C(t)$, \mathbf{t} and \mathbf{n} , obey the relations $\mathbf{t} = \mathbf{x}_s = \partial\mathbf{x}/\partial s$ and $\kappa\mathbf{n} = -\mathbf{t}_s$. (The minus sign in this last expression results from a desire to identify the normal vector for a closed curve with the *exterior* unit normal for the region it bounds and to have the curvature κ non-negative for curves that are boundaries of convex regions.) Here $H = \kappa$ and $\Delta_S H = \kappa_{ss}$. If we let $\theta = \theta(s, t)$ be the counterclockwise angle to $\mathbf{t}(s, t)$ from a line parallel to a fixed x -axis, then, for an appropriate choice of the direction of increase of s , $\kappa(s, t) = \theta_s(s, t)$ and (1.3) becomes

$$v = \theta_{sss}. \tag{1.4}$$

Because $\mathbf{x}_s \cdot \mathbf{n} = 0$, we have $v = \mathbf{x}_t \cdot \mathbf{n}$, and (1.4) can be written

$$\mathbf{x}_t \cdot \mathbf{n} = \theta_{sss}. \tag{1.5}$$

As $\mathbf{t}_t = -\theta_t \mathbf{n}$ and $\mathbf{t}_s = -\theta_s \mathbf{n}$, successive differentiation of Eq. (1.5) yields

$$-\theta_t + \theta_s \mathbf{x}_t \cdot \mathbf{t} = \theta_{ssss}, \tag{1.6}$$

$$-\theta_{ts} + \theta_{ss} \mathbf{x}_t \cdot \mathbf{t} - \theta_s^2 \mathbf{x}_t \cdot \mathbf{n} = \theta_{sssss}. \tag{1.7}$$

In view of (1.5) and (1.6), Eq. (1.7) tells us that

$$\theta_{ss}\theta_t - \theta_s\theta_{ts} = \theta_s\theta_{sssss} - \theta_{ss}\theta_{ssss} + \theta_s^3\theta_{sss}. \tag{1.8}$$

This partial differential equation for the tangent angle at s for the curve $C(t)$ will play an important role in our discussion.

As we are considering cases in which θ has classical derivatives in s of order five, (1.4) tells us that when $C(t)$ is the boundary of a compact body,

$$\int_{C(t)} v(s, t) ds = 0. \tag{1.9}$$

This relation expresses the assertion that curvature driven diffusion in the perimeter of a two-dimensional body conserves the area of that body.

1.1. General theory of similarity solutions

A *similarity solution* of Eq. (1.8) is one for which there are functions $\tilde{\theta}$ and γ such that

$$\theta(s, t) = \tilde{\theta}(v), \quad v = s\gamma(t). \tag{1.10}$$

We shall use the prime sign to indicate derivatives of $\tilde{\theta}$ and γ . For each similarity solution there is a constant c such that

$$(\tilde{\theta}''''\tilde{\theta}' - \tilde{\theta}'''\tilde{\theta}'' + \tilde{\theta}''(\tilde{\theta}')^3)/(\tilde{\theta}')^2 = c, \tag{1.11}$$

and $-\gamma'/\gamma^5 = c$, i.e.,

$$\gamma(t) = (b + 4ct)^{-1/4} \tag{1.12}$$

with $b \geq 0$ a constant. Curves $C(t)$ corresponding to solutions with $c > 0$ expand in time, and those for which $c < 0$ contract in time. When $c = 0$, $\theta_t(s, t) = 0$ and the curve $C(t)$ either remains fixed or moves at constant velocity without changing shape. We refer to similarity solutions of (1.8) with $c > 0$, $c < 0$, and $c = 0$ as *expanding*, *contracting*, and *invariant*, respectively.

In terms of $\eta = \eta(v) = \tilde{\theta}'(v)$, i.e., $\eta(v) = \gamma(t)^{-1}\kappa(s, t)$, Eq. (1.11) becomes

$$\eta''''\eta - \eta'''\eta' + \eta''\eta^3 - c\eta^2 = 0. \tag{1.13}$$

At this point we wish to remark that although Eq. (1.8) was derived by considering curves that are boundaries of (two-dimensional) bodies, there are planar curves $C(t)$ for which the tangent angle is governed by that equation, i.e., which evolve by curvature driven diffusion along the curve, but which cannot be regarded as boundaries. Examples of such curves are shown in Fig. 1 (B and C). Each curve in that figure (which will be discussed later) corresponds to an expanding sim-

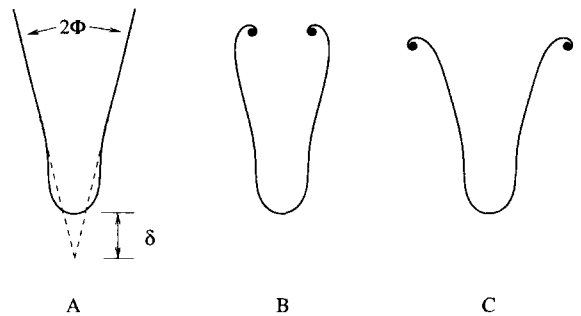


Fig. 1. Curves $C(t)$ at fixed t corresponding to symmetric expanding similarity solutions of Eq. (1.8). Each curve is determined by numerical solution of Eq. (2.2), i.e., of the system (2.6), with $\eta(0) = 1$, $\eta'(0) = \eta''(0) = 0$, and with values of $\eta''(0)$ that are (to 12 figures): (A) $\eta''(0) = -0.550291816458 = h_3^*[1]$, which, by (2.7) and (2.8), yields $\delta = 2.2012$ and $2\Phi = 27.10^\circ$; (B) $\eta''(0) = h_3^*[1] + 10^{-4}$; (C) $\eta''(0) = h_3^*[1] - 10^{-4}$.

ilarity solution of (1.8), but only the one labeled A represents the boundary of a planar (infinite) region.

Whether or not the time-dependent planar curve $C(t)$ is the boundary of a region, if $C(t)$ obeys (1.4) and the range of s is $(-\infty, +\infty)$, $C(t)$ satisfies (1.9) if and only if

$$\lim_{s \rightarrow \infty} \kappa_s(s, t) = \lim_{s \rightarrow -\infty} \kappa_s(s, t). \tag{1.14}$$

Later in the paper we shall be concerned with cases in which κ is an even function of s on $(-\infty, +\infty)$; in such cases (1.14) is satisfied if and only if

$$\lim_{s \rightarrow \infty} \kappa_s(s, t) = 0. \tag{1.15}$$

When Cartesian coordinates are employed and $C(t)$ has the representation $y = y(x, t)$, Eq. (1.3) takes the form [2],

$$y_t = -\frac{\partial}{\partial x} \left(\frac{\kappa_x}{\sqrt{1 + y_x^2}} \right), \quad \kappa = \frac{y_{xx}}{(1 + y_x^2)^{3/2}}, \tag{1.16}$$

or, equivalently,

$$(1 + y_x^2)^{-1/2} y_t(x, t) = -\kappa_{ss}(s, t). \tag{1.17}$$

Each solution of Eq. (1.16) for which

$$\tilde{y} = \tilde{y}(\tilde{x}) \quad \text{with} \quad \tilde{x} = \gamma(t)x, \quad \tilde{y} = \gamma(t)y \tag{1.18}$$

corresponds to a similarity solution of Eq. (1.8). The converse is not true in general: there are similarity solutions of (1.8) that cannot be written in the form (1.18). However, if the solution $\eta = \eta(v)$ of (1.13) is such that, as v varies over its full range, $\tilde{\theta}(v)$ is confined to an interval of length π , then, after an appropriate choice θ_0 of $\tilde{\theta}(0)$, integration of the function $\eta(\cdot)$ yields a similarity solution of Eq. (1.8) for which $\cos \tilde{\theta} > 0$ on the domain of $\tilde{\theta}(\cdot)$, and we can construct a solution $y = y(x, t)$ of Eq. (1.16) that obeys (1.18) (with $\gamma(t) = (b + 4ct)^{-1/4}$) by putting

$$\begin{aligned} \tilde{x}(v) &= \int_0^v \cos \tilde{\theta}(\xi) d\xi, \\ \tilde{y}(v) &= \int_0^v \sin \tilde{\theta}(\xi) d\xi + \tilde{y}(0), \\ \tilde{\theta}(v) &= \int_0^v \eta(\xi) d\xi + \theta_0, \end{aligned} \tag{1.19}$$

where $\tilde{y}(0)$ is arbitrary. (If such a value of θ_0 cannot be found, i.e., if the length of the range of θ exceeds π , it is not true that y can be expressed as a single-valued function of x and t .) We write \tilde{C} for the curve that has the parametric representation $\tilde{x} = \tilde{x}(\nu)$, $\tilde{y} = \tilde{y}(\nu)$ in the Cartesian system (\tilde{x}, \tilde{y}) . The arc-length coordinate for \tilde{C} is ν , and the curvature of \tilde{C} is $\eta = \eta(\nu)$. Once \tilde{C} is known, $C(t)$ is determined for each t for which $\gamma(t)$ is a positive number; our construction of \tilde{C} implies that the point on $C(t)$ with $s = 0$ is on the y -axis for each such t . In view of (1.17), (1.18) and (1.12), $\tilde{y}(\tilde{x})$ obeys

$$c(1 + \tilde{y}_x^2)^{-1/2}(\tilde{y} - \tilde{x}\tilde{y}_x) = -\eta_{\nu\nu}(\nu). \tag{1.20}$$

In this paper we shall discuss expanding similarity solutions of (1.8) for which curvature can be expressed as an even function of arc-length and that can be interpreted as describing the evolution of infinite wedges. Subsequent papers on similarity solutions will deal with invariant solutions, contracting solutions, and a special class of expanding solutions that appear to be of importance in extensions of the theory of thermal grooving formulated by Mullins in the paper [2] in which the field equation (1.3) of curvature driven surface diffusion first appeared. In the following section we shall present a procedure for finding, by numerical solution of equation (1.13), similarity solutions of (1.8) with specified asymptotic properties. This procedure differs from one, based on numerical integration of the Eq. (1.20), which was employed by Robertson [5] in a study of thermal grooving in cases in which a linearization introduced in [2] is not appropriate.

2. Expanding similarity solutions for diffusion along curves

For the case of expanding similarity solutions of (1.8), i.e., when $c > 0$ in (1.12), we can, without loss of generality, put $c = 1/4$ and $b = 0$ and thus obtain $\gamma(t) = t^{-1/4}$, and

$$\theta(s, t) = \tilde{\theta}(\nu), \quad \nu = st^{-1/4}, \tag{2.1}$$

$$\eta''''\eta - \eta'''\eta' + \eta''\eta^3 - \frac{1}{4}\eta^2 = 0. \tag{2.2}$$

The emphasis here is on cases in which the domain of $\eta(\cdot)$ and $\tilde{\theta}(\cdot)$ is infinite and $\tilde{x} \rightarrow \infty$ as $\nu \rightarrow \infty$. We are particularly interested in solutions of (2.2) for which

there is a time-invariant curve C^∞ with a representation of the form $y = g(x)$ and the property that, for each t , $C(t)$ is asymptotic to C^∞ for large x . When such is the case, g must either equal or be asymptotic to a function f that obeys the identity $\gamma f(x) = f(\gamma x)$ for $\gamma, x > 0$ and hence has the form $f(x) = Ax$. Thus, we shall seek expanding similarity solutions of Eq. (1.8) for which $C(t)$ for each t is asymptotic to an invariant straight line that passes through the origin of a Cartesian coordinate system in which (1.18) holds. A plausible place to start the search for such solutions of Eq. (1.8) is among the solutions of Eq. (2.2) for which

$$\lim_{\nu \rightarrow \infty} \eta(\nu) = 0. \tag{2.3}$$

The solutions that we can find obeying this condition are also such that $\eta', \eta'', \eta''' \rightarrow 0$ as $\nu \rightarrow \infty$ and hence obey the relation (1.15).

One way to write Eq. (2.2) as a system is to put

$$\zeta' = \mathbf{f}(\zeta), \quad \zeta = (\zeta_1, \zeta_2, \zeta_3, \zeta_4) = (\eta, \eta', \eta'', \eta'''). \tag{2.4}$$

However, for a solution η of Eq. (2.2) on $(0, \infty)$ that obeys (2.3), there are generally values ν^* of ν at which $\eta'(\nu^*) = \eta''(\nu^*)\eta'(\nu^*) = 0$, and, as the fourth component of ζ' , i.e., $\zeta_4' = \eta'''' = (\eta''')'$, contains a term of the form $\zeta_4\zeta_2/\zeta_1 = \eta'''\eta'/\eta$, $\mathbf{f}(\zeta(\nu))$ is not well defined where $\nu = \nu^*$. To overcome this difficulty, we write Eq. (2.2) in the form $\mathbf{h}' = \mathbf{g}(\mathbf{h})$, where $\mathbf{h} = (h_1, h_2, h_3, h_4)$ with

$$h_1 = \eta, \quad h_2 = \eta', \quad h_3 = \eta'', \quad h_4 = \eta\eta' + \eta''/\eta, \tag{2.5}$$

and so obtain a system that is well defined and locally Lipschitzian for all values of \mathbf{h} :

$$\begin{aligned} h_1' &= h_2, & h_2' &= h_3, & h_3' &= h_4h_1 - h_1^2h_2, \\ h_4' &= \frac{1}{4} + h_2^2. \end{aligned} \tag{2.6}$$

2.1. Symmetric curves asymptotic to invariant lines

We are interested in solutions of (2.2) for which $\eta(\cdot)$ is an even function. We call such a solution *symmetric* because for it the curve \tilde{C} has a line l^0 of symmetry

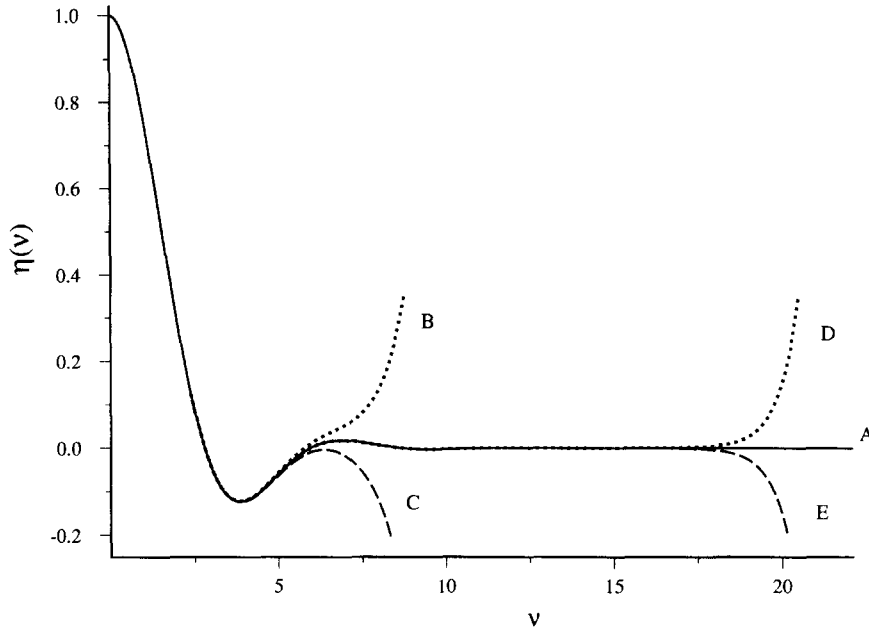


Fig. 2. Solutions $\eta(v) = h_1(v)$ of the system (2.6) with $h_1(0) = \eta_0 = 1$, $h_2(0) = h_4(0) = 0$: (A) $h_3(0) = h_3^*$; (B) $h_3(0) = h_3^* + 10^{-4}$; (C) $h_3(0) = h_3^* - 10^{-4}$; (D) $h_3(0) = h_3^* + 10^{-12}$; (E) $h_3(0) = h_3^* - 10^{-12}$.

(which passes through the point $v = 0$ and is parallel to $\mathbf{n}(0)$). Such curves \tilde{C} are shown in Fig. 1. Our interest is in cases for which \tilde{C} is asymptotic to a straight line l^+ as $v \rightarrow \infty$ and hence to a straight line l^- as $v \rightarrow -\infty$, as in Fig. 1(A). We place the origin \mathbf{O} of the system (\tilde{x}, \tilde{y}) at the intersection of l^+ and l^- and choose the \tilde{y} -axis to be the line l^0 of symmetry, which yields not only $\theta_0 = 0$ in (1.19), but also $\tilde{y}_{\tilde{x}}(0) = 0$ in (1.20) and hence

$$\delta = -4\eta_{vv}(0). \tag{2.7}$$

where $\delta = \tilde{y}(0)$ is the distance from \mathbf{O} to \tilde{C} . If we write 2Φ for the angle between l^+ and l^- , then

$$\Phi = \pi/2 - \lim_{v \rightarrow \infty} \tilde{\theta}(v) = \pi/2 - \int_0^{\infty} \eta(v) dv. \tag{2.8}$$

To find \tilde{C} when Φ is given, we employ an inverse method in which we first determine the dependence of solutions of (2.4) on $\eta(0)$ and then use (2.8) to obtain a graph of Φ vs. $\eta(0)$. As η is here an even function, it suffices to solve (2.4) for $v \geq 0$, and in the initial data for the system (2.4), i.e., in $\zeta(0) = (\eta(0), \eta'(0), \eta''(0), \eta'''(0))$, we have $\eta'(0) =$

$\eta'''(0) = 0$. To find η as a function of v for a given value η_0 of $\eta(0)$ we seek the value η''_0 of $\eta''(0)$ such that the (unique) solution $\mathbf{h}(\cdot)$ of the system (2.6) with the initial data $\mathbf{h}(0) = (h_1(0), h_2(0), h_3(0), h_4(0)) = (\eta_0, 0, \eta''_0, 0)$ is such that $\eta(\cdot)$, i.e., $h_1(\cdot)$, has the asymptotic property (2.3). We have used a shooting procedure for computing approximations to η''_0 . As the procedure is based on the system (2.6) in which $h_3(v) = \eta''(v)$, we denote the approximations to η''_0 obtained from it by h_3^* . For a given η_0 , $h_3^* = h_3^*[\eta_0]$ is taken to be the value of $h_3(0)$ that yields the longest range of v on which $|\mathbf{h}(v)|$ is small.

Several fourth-order and fifth-order numerical methods of Runge–Kutta and predictor–corrector type were used to integrate the system (2.6). For each choice of the initial datum $\eta_0 = h_1(0)$ and the integration method, a value of h_3^* was computed to 16 significant figures. We found h_3^* to be independent of the integration method to 12 significant figures for step sizes Δv with maximum values less than 10^{-3} .

A typical example of our numerical calculations is illustrated in Fig. 2, where $\eta_0 = 1$. The heavy solid curve there labeled A is the graph η vs. v corresponding to the best approximation $h_3^*[1]$ we found for η''_0 . The dashed and dotted curves shown in the figure

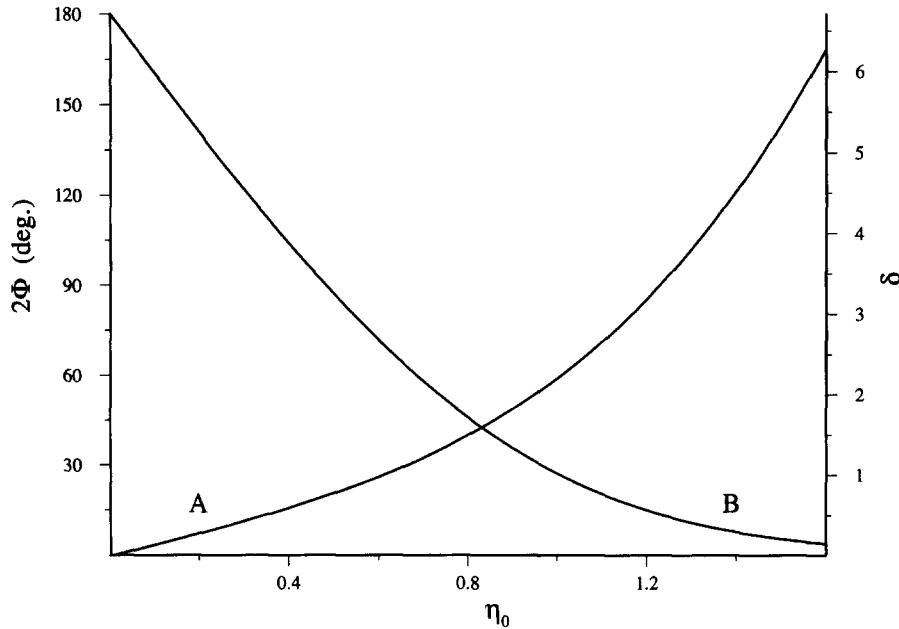


Fig. 3. Graphs of the following functions of η_0 for wedges evolving by curvature driven surface diffusion: (A) δ , given by (2.7); (B) the angle of aperture 2Φ .

illustrate the effects of perturbations to $h_3^*[1]$ and confirm the general rule that the better the approximation to η_0'' , the longer the interval of values of ν on which $|h(\nu)|$ remains small. In this case we find that if $h_3(0) = h_3^*$, then $|h_1(\nu)| < 10^{-4}$ for $13 < \nu < 21$. That h_3^* is only an approximation to η_0'' becomes clear when the solution is extended beyond the range shown in the figure; our best value h_3^* yields values of $|h_1(\nu)|$ that increase monotonically with ν for $\nu > 22$ and surpass 0.1 at $\nu = 25$.

The first component $h_1(\cdot) = \eta(\cdot)$ of the solution h of (2.6) corresponding to the best value $h_3^*[\eta_0]$ we can obtain for η_0'' gives us the curve \tilde{C} by (1.19) and the angle $\Phi = \Phi(\eta_0)$ by (2.8). The number h_3^* gives an approximation to $\delta = \delta(\eta_0)$, for, by (2.7), $\delta(\eta_0) = -4\eta_0''$. Graphs of δ and 2Φ vs. η_0 are shown in Fig. 3.

In Fig. 1, we show curves \tilde{C} corresponding to the graphs of η vs. ν labeled A, B, C in Fig. 2. The curves labeled B and C in Fig. 1 illustrate the importance of having a good approximation to η_0'' .

The curves \tilde{C} shown in Fig. 4 correspond to selected values of 2Φ and were computed in the following way: the data used to construct graph B of Fig. 3 were

employed to obtain a value of η_0 for each specified value of 2Φ , and for that η_0 the data used to construct graph A of Fig. 3 gave the corresponding value of $h_3^*[\eta_0]$. From the pair $(\eta_0, h_3^*[\eta_0])$, η as a function of ν was computed by numerical integration of (2.6), and the Cartesian coordinates of the points on \tilde{C} were calculated from (1.19). In view of (2.1), (1.19) and (1.18), \tilde{C} can be identified with $C(t)$ for $t = 1$, and for each $t > 0$ the curve $C(t)$ is the magnification of $C(1)$ by the factor of $t^{1/4}$. In cases such as these, for which \tilde{C} does not cross itself and is asymptotic to straight lines l^+ and l^- as $\nu \rightarrow +\infty$ and $-\infty$, $C(t)$ can be regarded as the boundary at time t of an infinite solid body B.

We take the range of Φ to be the open interval $(0, \pi/2)$. For Φ in that interval, as $t \rightarrow 0+$, $C(t)$ approaches the lines l^+ and l^- uniformly in s for $-\infty < s < \infty$. In other words, the function $t \mapsto C(t)$ describes the evolution for $t > 0$ of the boundary of a body that in the limit $t \rightarrow 0+$ has the form of an infinite wedge W with angle of aperture 2Φ .

Because the relations (1.14) and (1.15) hold here, Eq. (1.9) implies that the signed area between $C(t)$

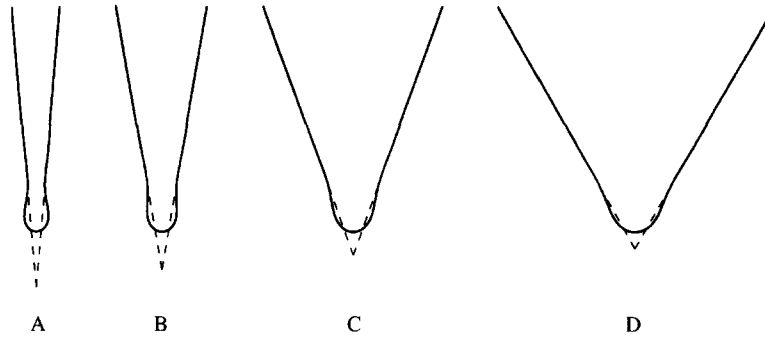


Fig. 4. Curves \tilde{C} corresponding to symmetric expanding similarity solutions of Eq. (1.8) which governs curvature driven surface diffusion: (A) $2\Phi = 10^\circ$, $\delta = 3.98$; (B) $2\Phi = 20^\circ$, $\delta = 2.64$; (C) $2\Phi = 40^\circ$, $\delta = 1.64$; (D) $2\Phi = 60^\circ$, $\delta = 1.17$.

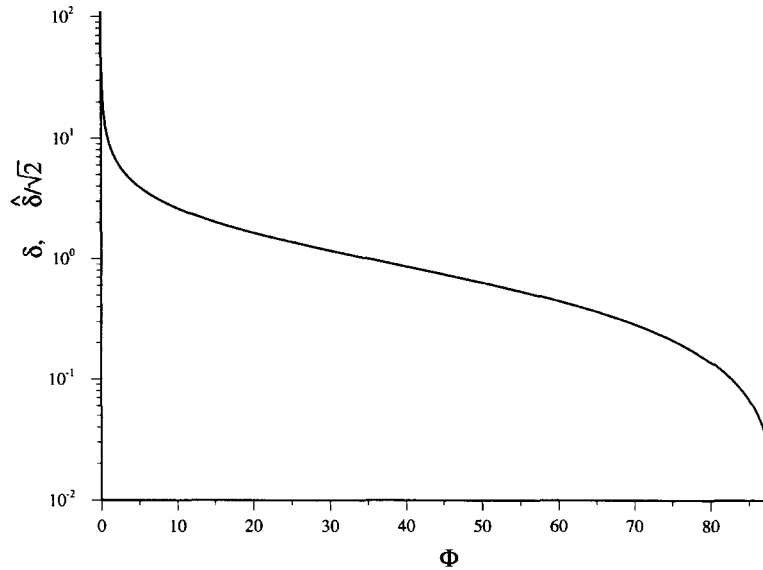


Fig. 5. The relation between Φ and the dimensionless numbers δ and $\hat{\delta}$ that determine, by (2.10) and (3.31), respectively, the retraction $\Delta(t)$ of the tip of a wedge. In the theory of curvature driven surface diffusion δ obeys Eq. (2.7). In the theory of curvature driven evaporation $\hat{\delta}$ obeys Eq. (3.24) and its equivalent (3.35). Comparison of the results of numerical integration of (2.2) with evaluation of the integrals in (3.24), (3.25) indicates a remarkable coincidence of the graphs of δ and $\hat{\delta}/\sqrt{2}$ vs. Φ .

and its asymptotes must be zero for all $t > 0$. This fact gives us a further check on the reliability of our numerical methods. For $0 < \eta_0 < 1.6$, we have found the ratio of the signed area to the absolute area of the region between the calculated curve \tilde{C} and its asymptotes to be less than 10^{-3} .

The retraction $\Delta(t) = y(0, t)$, i.e., the distance from the point $s = 0$ on $C(t)$ to the intersection of the fixed asymptotic lines l^+ and l^- , is given by

$$\Delta(t) = t^{1/4} \delta. \tag{2.9}$$

In conventional (e.g., SI) units, Eq. (2.9) becomes

$$\Delta(t) = (Kt/\rho)^{1/4} \delta. \tag{2.10}$$

Although δ is the dimensionless quantity constructed using (an arbitrary) characteristic length L as the unit of length, that length does not appear in either (2.9) or (2.10). This is not surprising, for $C(t)$ evolves by similarity transformations.

A graph δ vs. Φ , based on Eqs. (2.7) and (2.8), is given in Fig. 5. In the following section we shall give evidence to the effect that the relation between δ and

Φ has the analytic representation:

$$\begin{aligned} \Phi &= \frac{\pi}{2} - \int_0^{\delta/\sqrt{2}} \frac{d\eta}{[\delta^2/2 - \eta^2 + \ln(\delta/\sqrt{2}\eta)]^{1/2}} \\ &= \int_{\delta/\sqrt{2}}^{\infty} \frac{dR}{R[(R^2/2\delta^2)e^{(R^2/2-\delta^2)} - 1]^{1/2}}. \end{aligned} \tag{2.11}$$

3. Similarity solutions in the theory of curvature driven evaporation

The expanding similarity solutions just presented for the theory of motion by curvature driven diffusion along curves have analogs in the theory of motion by evaporation and condensation. For a planar curve $C(t)$, the basic equation of the latter theory (generally referred to as the theory of *motion by curvature*) is $v = -k\kappa$, with k a positive material constant [3]. If one uses, instead of t and x, y, s , etc., the dimensionless variables kt/L^2 and $x/L, y/L, s/L$, (for which we shall here write t, x, y, s, \dots), the equation becomes

$$v = -\kappa \tag{3.1}$$

and gives the following analog of (1.5):

$$\mathbf{x}_t \cdot \mathbf{n} = -\theta_s. \tag{3.2}$$

The argument by which we derived (1.8) from (1.5) tells us that (3.2) is equivalent to the following partial differential equation for the tangent angle $\theta = \theta(s, t)$:

$$\theta_{ss}\theta_t - \theta_s\theta_{st} = \theta_{ss}^2 - \theta_s^4 - \theta_s\theta_{sss}. \tag{3.3}$$

For a similarity solution, i.e., one with the form

$$\theta(s, t) = \tilde{\theta}(v), \quad v = s\gamma(t), \tag{3.4}$$

(3.3) yields

$$(\tilde{\theta}''^2 - \tilde{\theta}'^4 - \tilde{\theta}'\tilde{\theta}''')/(\tilde{\theta}')^2 = c \tag{3.5}$$

and

$$\gamma(t) = (b + 2ct)^{-1/2}, \tag{3.6}$$

with $b \geq 0$. As in the case of curvature driven diffusion, expanding, contracting and invariant solutions correspond, respectively, to $c > 0, c < 0$, and $c = 0$.

If we put, as in Section 1, $\eta = \eta(v) = \tilde{\theta}'(v)$, we here have $\eta(v) = \gamma(t)^{-1}\kappa(s, t)$ and, in place of (1.13), an equation,

$$\eta\eta'' - \eta'^2 + \eta^4 + c\eta^2 = 0, \tag{3.7}$$

whose solution can be rendered explicit. If there is a finite value of v at which $\eta(v) = 0$, then (3.7) implies that $\eta(v) = 0$ for all v and $C(t)$ is (an invariant) straight line. If not, we may take $\eta(v)$ to be positive for all v and note that the first integral of (3.7) then has the form

$$(\eta'/\eta)^2 = \alpha - \eta^2 - 2c \ln \eta \tag{3.8}$$

with α a constant obeying

$$\alpha \geq \inf_{\eta > 0} (\eta^2 + 2c \ln \eta). \tag{3.9}$$

(Of course, for $c > 0$ the relation (3.9) places no constraint on α). When η is not everywhere 0, we choose the point $v = 0$ such that $\eta(0) = \eta_0$ with η_0 a root of the equation

$$\eta^2 + 2c \ln \eta = \alpha; \tag{3.10}$$

we then have $\eta'(0) = 0$, the solution of (3.7) takes the form

$$v = v(\eta) = \pm \int_{\eta_0}^{\eta} \frac{d\eta}{\eta[\eta_0^2 - \eta^2 + 2c \ln(\eta_0/\eta)]^{1/2}}, \tag{3.11}$$

and η is an even function of v . Thus *each* similarity solution of (3.3) corresponds to a *symmetric* time-dependent curve $C(t)$.

If $c < 0$ and equality holds in (3.9), the root η_0 of (3.10) is unique, the solution of (3.8) is a constant equal to η_0 , and, for $t < -b/(2c)$, the curve $C(t)$ is a circle of radius $R(t) = \eta_0^{-1}(b + 2ct)^{1/2}$. If, for $c < 0$, (3.9) is an inequality, then (3.10) has two distinct roots $\eta_0^{(1)}, \eta_0^{(2)}$ for each α obeying (3.9); the solution of (3.7) for each such α is periodic, and $\eta_0^{(1)}, \eta_0^{(2)}$ correspond to the maximum and minimum values of η . For $c \geq 0$ the root η_0 of (3.10) is unique for each α obeying (3.9), and the corresponding solution η of (3.7) is an even function that is monotone decreasing on $[0, \infty]$ with $\eta(v) \rightarrow 0$ as $v \rightarrow \infty$.

Here, as in Section 2, we take the x -axis to be perpendicular to a line l° of symmetry for the curve $C(t)$; hence $\tilde{\theta}(0) = 0$ and

$$\tilde{\theta}(v) = \int_0^v \eta(v) dv. \tag{3.12}$$

When $c \geq 0$, l° is unique, and one can show that, by (3.11),

$$\begin{aligned} \lim_{v \rightarrow \infty} \tilde{\theta}(v) &= \int_0^\infty \eta(v) dv \\ &= \int_0^{\eta_0} \frac{d\eta}{[\eta_0^2 - \eta^2 + 2c \ln(\eta_0/\eta)]^{1/2}}. \end{aligned} \tag{3.13}$$

The above integral is finite for each $\eta_0 > 0$. It follows that every expanding and invariant similarity solution of Eq. (3.3) for which \tilde{C} is not a straight line is such that \tilde{C} is asymptotic to straight lines l^+ and l^- as $v \rightarrow +\infty$ and $v \rightarrow -\infty$. The angle 2Φ of intersection of l^+ and l^- is

$$\Phi = \pi/2 - \tilde{\theta}(\infty), \tag{3.14}$$

where $\tilde{\theta}(\infty)$ stands for $\lim_{v \rightarrow \infty} \tilde{\theta}(v)$ and is given by (3.13).

For invariant solutions, i.e., when $c = 0$, without loss of generality we can put $b = 1$ in (3.6). We then have $v = s$, $\eta = \kappa$, and the integral in (3.11) reduces to

$$s(\kappa) = \pm \int_{\kappa_0}^{\kappa} \frac{d\kappa}{\kappa \sqrt{\kappa_0^2 - \kappa^2}}, \tag{3.15}$$

which yields an explicit relation between $\kappa(s)$ and the maximum value $\kappa_0 = \kappa(0)$ attained by the curvature:

$$\kappa(s) = \frac{\kappa_0}{\cosh(\kappa_0 s)}. \tag{3.16}$$

For $c = 0$, (3.14) yields $\Phi = 0$, which says that invariant solutions produce curves that are asymptotic to parallel lines. As we discuss below, invariant solutions of Eq. (3.3) that do not correspond to straight lines undergo a translation at constant velocity along the symmetry axis l° .

In the seminal paper on the theory of Eq. (3.1), Mullins [3] pointed out that when $C(t)$ has a polar coordinate representation $r = r(\varphi, t)$, Eq. (3.1) becomes

$$rr_t = -\frac{r^2 + 2r_\varphi^2 - rr_{\varphi\varphi}}{r^2 + r_\varphi^2}. \tag{3.17}$$

Mullins called solutions of this equation for which

$$r(\varphi, t) = R(\varphi)T(t) \tag{3.18}$$

invariant under magnification and showed that for them

$$T(t) = \gamma(t)^{-1} \tag{3.19}$$

with $\gamma(t)$ as in (3.6). When $c \neq 0$ and $C(t)$ has a polar coordinate representation $r = r(\varphi, t)$, our concept of a similarity solution of (3.3) is equivalent to the concept of a solution of (3.17) invariant under magnification.

Similarity solutions of (3.3) with $c = 0$ that do not reduce to $\eta(v) \equiv 0$ are not solutions of (3.17) obeying (3.18), but are instead of a type that Mullins called *invariant under translation*. The curves corresponding to these solutions have the Cartesian coordinate representation (viz. [3, p. 903]):

$$y = y(x, t) = Vt - V^{-1} \ln \cos(Vx). \tag{3.20}$$

Such a curve advances along the y -axis with constant velocity V ; its curvature $\kappa(s)$ is given by the invariant (i.e., $c = 0$) solution (3.16) of Eq. (3.7). In the dimensionless units we are using here, the velocity V in (3.20) equals κ_0 in (3.16), and V^{-1} is the distance between the fixed parallel lines l^+ , l^- to which $C(t)$ is asymptotic for each t .

In general, when $C(t)$ has the Cartesian representation $y = y(x, t)$, Eq. (3.1) takes the form [3]:

$$(1 + y_x^2)^{-1/2} y_t = \kappa, \quad \kappa = \frac{y_{xx}}{(1 + y_x^2)^{3/2}}. \tag{3.21}$$

Each solution of this last equation for which (1.18) holds with $\gamma(t)$ as in (3.6) corresponds to a similarity solution of (3.3) and can be constructed from the function $\eta(\cdot)$ using (1.19) with $\theta_0 = 0$. For such solutions of (3.21), $\tilde{y}(\tilde{x})$ obeys

$$\begin{aligned} c(1 + \tilde{y}_x^2)^{-1/2} (\tilde{y} - \tilde{x} \tilde{y}_x) &= \eta, \\ \eta &= \frac{\tilde{y}_{\tilde{x}\tilde{x}}}{(1 + \tilde{y}_{\tilde{x}}^2)^{3/2}}. \end{aligned} \tag{3.22}$$

Of principal interest here are expanding similarity solutions; for them, without loss of generality, we put $c = 1/2$ and $b = 0$ to obtain $\gamma(t) = t^{-1/2}$, $v = t^{-1/2}s$, and $\eta(v) = t^{1/2}\kappa(s, t)$. As in Section 2, we place the origin \mathbf{O} of the (\tilde{x}, \tilde{y}) -coordinate system at the intersection of l^+ and l^- , which, together with the fact that $\tilde{\theta}(0) = 0$, implies that in Eq. (3.21) we have $\tilde{y}_{\tilde{x}}(0) = 0$, and hence

$$2\eta(0) = \tilde{y}(0) = \hat{\delta}, \tag{3.23}$$

where $\hat{\delta}$ is, as in (2.7), the distance in the (\tilde{x}, \tilde{y}) -plane between \mathbf{O} and the point on \tilde{C} with $v = 0$. Thus, for expanding similarity solutions of (3.3), we have, by (3.13) and (3.14), a surprisingly simple relation between $\hat{\delta}$ and the angle of aperture 2Φ :

$$2\Phi = \pi - 2 \int_0^{\hat{\delta}/2} \frac{d\eta}{[\hat{\delta}^2/4 - \eta^2 + \ln(\hat{\delta}/2\eta)]^{1/2}}. \tag{3.24}$$

In this theory, the retraction $\hat{\Delta}(t) = y(0, t)$, i.e., the time-dependent distance between $C(t)$ and the intersection of the fixed asymptotic lines l^+ and l^- , is given by

$$\hat{\Delta}(t) = t^{1/2}\hat{\delta}(\Phi). \tag{3.25}$$

In a paper [6] on grain boundary motion by curvature driven evaporation, Sun and Bauer observed that a functional relation of a general type (3.25) must hold. They stated that the specific function $\hat{\delta}(\Phi)$ ‘cannot be expressed analytically’, but calculated it by a finite difference scheme applied to a partial differential equation equivalent to (3.17). The graph of their numerical results agrees with our explicit expression (3.24) for $\Phi(\hat{\delta})$ (and hence with the equivalent expression (3.35) below).

Eq. (3.11) here yields

$$v = \pm \int_{\hat{\delta}/2}^{\eta} \frac{d\eta}{[\hat{\delta}^2/4 - \eta^2 + \ln(\hat{\delta}/2\eta)]^{1/2}}. \tag{3.26}$$

In a study of the evolution of surface grooves by curvature driven evaporation and condensation, Broadbridge [7] obtained a solution of Eq. (3.22) (with $c > 0$) equivalent to Eq. (3.26). The relation (3.24) is not mentioned in [7], for the boundary conditions appropriate to the problems treated are different from those occurring here.

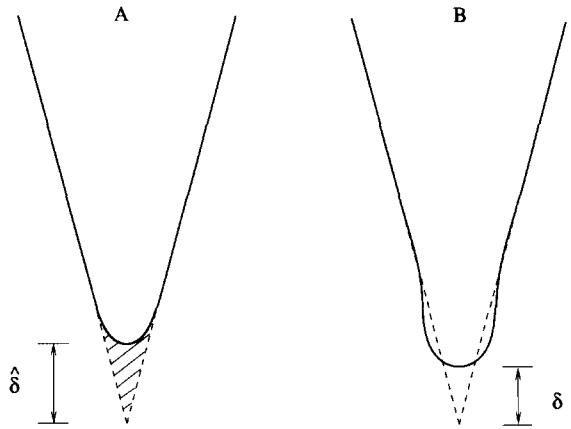


Fig. 6. Profiles of wedges with angle of aperture $2\Phi = 30^\circ$ that are evolving by (A) curvature driven evaporation; (B) curvature driven surface diffusion.

Eqs. (3.26) and (3.24) permits us to draw the curve \tilde{C} for a specified value of 2Φ . We can again identify \tilde{C} with $C(1)$; here, $C(t)$ is the magnification of $C(1)$ by the factor of $t^{1/2}$. Curves $C(t)$ obtained this way describe the evolution of a wedge with angle of aperture 2Φ by curvature driven evaporation. The case in which $2\Phi = 30^\circ$ is shown in Fig. 6, where it may be compared with our results for the same angle of aperture in the theory of Section 2. (The curves \tilde{C} seen in Figs. 6(A) and 7(A–C) were drawn using Eq. (3.34) below, which is equivalent to (3.26) and simplifies calculation of \tilde{C} .) It will be noticed that in the theory of (3.1), the convexity of the original wedge (defined by the dashed lines) is preserved in time. Huisken proved his theorem about conservation of convexity for motion by curvature assuming that the evolving surface is closed and compact. We have here an example in which the curve is not compact. Among the curves shown in Fig. 7 for several values of Φ is one (D) corresponding to the invariant solution (3.20). Although this curve undergoes a motion of translation, rather than expansion, it appears here as a limit for small Φ of curves \tilde{C} corresponding to expanding solutions of (3.3). This is a consequence of the fact that if we put $\gamma_c(t) = (1 + 2ct)^{-1/2}$, $v = s\gamma_c(t)$, $\eta(v) = \gamma_c(t)^{-1}\kappa(s, t)$, then, as we let c approach 0 from above with η_0 held fixed in the solution (3.11) of (3.7), we have not only $\gamma_c(t) \rightarrow 1$ and $v \rightarrow s$, but also $\eta(v) \rightarrow \kappa(s)$, where $\kappa(s)$ obeys (3.16) with κ_0 the fixed value of η_0 .

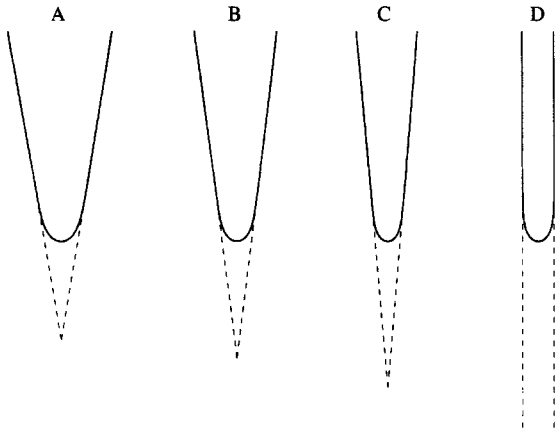


Fig. 7. Curves \tilde{C} corresponding to expanding similarity solutions of Eq. (3.3) governing curvature driven evaporation: (A) $2\Phi = 20^\circ$, $\hat{\delta} = 3.73$; (B) $2\Phi = 15^\circ$, $\hat{\delta} = 4.45$; (C) $2\Phi = 10^\circ$, $\hat{\delta} = 5.63$. (D) The curve $C(t)$ corresponding to the invariant solution (3.16) with $\kappa_0 = 2.5$.

The area $A(t)$ of the region bounded by $C(t)$ and the asymptotic lines l^+ , l^- (e.g., of the shaded region in Fig. 6(A)) obeys the relation

$$\frac{dA}{dt} = - \int_{-\infty}^{\infty} v ds. \tag{3.27}$$

Hence, when the motion is caused by curvature driven evaporation, (3.1) yields

$$\frac{dA}{dt} = \int_{-\infty}^{\infty} \kappa ds = 2 \int_0^{\infty} \kappa ds = 2[\theta(\infty, t) - \theta(0, t)]; \tag{3.28}$$

and, as $A(0) = 0$, $\theta(0, t) = 0$, and $\theta(\infty, t) = \pi/2 - \Phi$, we have

$$A(t) = (\pi - 2\Phi)t. \tag{3.29}$$

In other words, the amount of material lost to its environment by a wedge with angle of aperture 2Φ that has been evolving since $t = 0$ by curvature driven evaporation is, in conventional units,

$$A = (\pi - 2\Phi)kt. \tag{3.30}$$

In the same units, the retraction of the wedge tip is

$$\hat{\Delta}(t) = (kt)^{1/2} \hat{\delta}(\Phi). \tag{3.31}$$

One can calculate the curves \tilde{C} for expanding similarity solutions of (3.3) by another approach. When $C(t)$ has a polar coordinate representation $r = r(\varphi, t)$ with $r(\varphi, t) = R(\varphi)/\gamma(t)$, and $c = 1/2$ in (3.6), Eq. (3.17) yields

$$R^2 + 2R'^2 - RR'' + \frac{1}{2}R^4 + \frac{1}{2}R^2R'^2 = 0. \tag{3.32}$$

The above equation has the first integral,

$$(R'/R)^2 = \beta R^2 e^{R^2/2} - 1, \tag{3.33}$$

with β as constant. If we again place the origin at the intersection of the asymptotic lines l^+ and l^- and choose the line $\varphi = 0$ as the line l° of asymmetry for \tilde{C} (i.e., as the \tilde{y} -axis), then $R'(0) = 0$, $R(0) = R_0 = \hat{\delta}$, and (3.33) yields $\beta^{-1} = R_0^2 e^{R_0^2/2}$ and

$$\varphi(R) = \pm \int_{R_0}^R \frac{dR}{R[(R^2/R_0^2)e^{(R^2-R_0^2)/2} - 1]^{1/2}}. \tag{3.34}$$

It follows from (3.34) that the angle Φ that the asymptotes make with the line of symmetry $\varphi = 0$ is given as a function of $\hat{\delta}$ by

$$\Phi(\hat{\delta}) = \int_{\hat{\delta}}^{\infty} \frac{dR}{R[(R^2/\hat{\delta}^2)e^{(R^2-\hat{\delta}^2)/2} - 1]^{1/2}}, \tag{3.35}$$

which is equivalent to Eq. (3.24). One may use either (3.26) or (3.34) to obtain the curves \tilde{C} of the type shown in Figs. 6(A) and 7(A–C). Use of (3.34) permits one to avoid numerical evaluation of the three integrals in (1.19).

We believe that Eqs. (3.24) and (3.35), giving Φ as a function of $\hat{\delta}$, are new. The principal result of this study is summarized in the caption to Fig. 5. We have observed that, within the precision with which we are able to integrate the governing equations of the theory of curvature driven diffusion along the curves, the graph of δ vs. Φ obtained by the methods described in Section 2 appears to coincide with the graph of $\hat{\delta}/\sqrt{2}$ vs. Φ based on the Eqs. (3.24) and (3.35). If the graphs do indeed coincide, i.e., if the relation

$$\delta(\Phi) = \hat{\delta}(\Phi)/\sqrt{2}, \tag{3.36}$$

or, equivalently (2.11), holds exactly, it is an interesting result, because the theories of motion by curvature

driven surface diffusion and curvature driven evaporation give rise to time-dependent curves $C(t)$ that differ in such qualitative properties as convexity and conservation of area.

Added note (February 1998):

After this paper was submitted for publication in May 1997, the paper listed below as [8] was published and seen by us. In [8] similarity solutions obtained by a numerical procedure differing from the present are employed to describe the motion resulting from curvature driven diffusion in the surface of a solid film wedge on a substrate, and a detailed discussion is given of physical applications of wedge-like similarity solutions. A film wedge making a contact angle β with a substrate obeys the theory developed here when $\beta = 90^\circ$.

Graphs of δ vs. Φ are presented in Fig. 10 of [8] for $\beta = 90^\circ$, 135° , and 180° . These appear to be piecewise linear approximations based on calculated data points spaced by 10° in Φ . The corresponding problem in the theory of curvature driven evaporation is not examined there, and hence the present relation (3.36) between results of the two theories is not given.

As is remarked in [8], for sufficiently small values of Φ the theory of curvature driven surface diffusion yields a curve \tilde{C} that intersects itself and can no longer be interpreted as a boundary of a wedge-like region. We found that self-intersections of \tilde{C} occur when Φ is in the interval $0 < \Phi < 0.190^\circ$, which appears to agree with Fig. 5 of [8]. (In the theory of curvature driven evaporation, our exact expressions (3.34) and (3.35) imply that \tilde{C} does not intersect itself for any $\Phi > 0$.)

The calculations of $\Phi(\delta)$ that we performed to verify the validity of the relation (3.36) between

solutions of two differential equations were deliberately extended as far as feasible into the range near $\Phi = 0^\circ$ that is non-physical (for the fourth-order equation) and were such that the interval between successive values of Φ varied from 3×10^{-4} to 5×10^{-1} degrees, with that interval smallest for Φ near to 0° .

Acknowledgements

We are grateful to Alberto Cuitiño and David Swigon for the valuable discussions. This research was supported by the National Science Foundation under Grants DMS-94-04580 and DMS-94-03552.

References

- [1] C. Herring, Surface diffusion as a motivation for sintering, in: W.E. Kingston (Ed.), *The Physics of Powder Metallurgy*, McGraw Hill, New York, 1951, 143–179.
- [2] W.W. Mullins, Theory of thermal grooving, *J. Appl. Phys.* 28 (1957) 333–339.
- [3] W.W. Mullins, Two-dimensional motion of idealized grain boundaries, *J. Appl. Phys.* 27 (1956) 900–904.
- [4] G. Huisken, Flow by mean curvature of convex surfaces into spheres, *J. Diff. Geom.* 20 (1984) 237–266.
- [5] W.M. Robertson, Grain-boundary grooving by surface diffusion for finite surface slopes, *J. Appl. Phys.* 42 (1971) 463–467.
- [6] R.C. Sun, C.L. Bauer, Measurements of grain boundary mobilities through magnification of capillary forces, *Acta Met.* 18 (1970) 635–638.
- [7] P. Broadbridge, Exact solvability of the Mullins nonlinear diffusion model of groove development, *J. Math. Phys.* 30 (1989) 1648–1651.
- [8] H. Wong, M.J. Miksis, P.W. Voorhees, S.H. Davis, Capillarity driven motion of solid film wedges, *Acta Mater.* 45 (1997) 2477–2484.